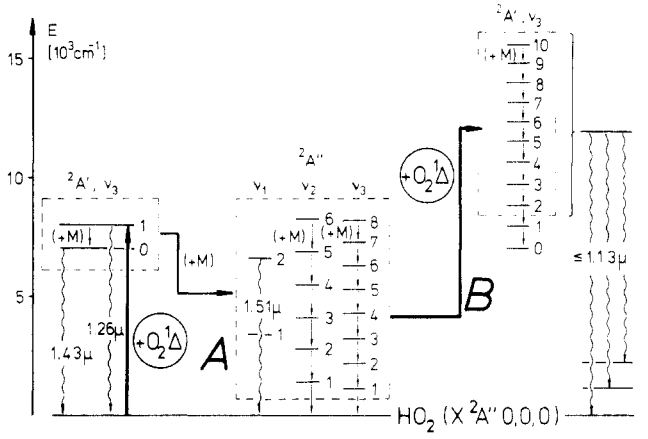

Figure 7. Excitation and relaxation processes of $HO_2(^2A',\nu_3')$ in $HO_2/O_2(^1\Delta)$ mixtures.

(A) which is driven by the reaction of the fairly long-lived radical HO_2 and the very long-lived energy carrier $O_2(^1\Delta)$. Process A can take place as long as $O_2(^1\Delta)$ is still present in the reaction mixture. It is probably responsible for most of the $HO_2(^2A')$ emissions at 1.43 and 1.26 μm which are observed in the reaction of many molecules, including methanol and allyl alcohol, with microwave-discharged oxygen. A side path B then populates the higher vibrationally excited levels of the electronically excited $HO_2(^2A')$ which are responsible for the 800–1200-nm emission of HO_2 described in the present work.

Conclusions

The ν_3 sequences of the $HO_2(A^2A' \rightarrow X^2A'')$ electronic transition have been observed up to $\Delta v_3 = 6$ between 800 and 1600 nm. Two mechanisms are suggested in order to explain the formation of these highly excited HO_2 molecules:

(1) In gas mixtures containing HO_2 and $O_2(^1\Delta)$ the previously suggested excitation reaction 1 takes place, and considerable concentrations of vibrationally excited ground-state molecules are populated during the relaxation of $HO_2(^2A')$. Part of these vibrationally excited molecules are then excited by a second $O_2(^1\Delta)$ molecule populating high vibrationally excited ν_3' levels of the electronically excited $^2A'$ state.

(2) $HO_2(^2A',v_3' \leq 6)$ is formed during the thermal $H + O_2$ recombination, possibly by collision-induced $V \rightarrow E$ energy transfer from vibrationally excited ground-state molecules.

There is no evidence from this work that the formerly suggested reaction 3 of HCO with $O_2(^1\Delta)$ represents an important source of $HO_2(^2A')$ molecules.

Acknowledgment. Financial support of this work by the Deutsche Forschungsgemeinschaft (SFB 42) and the Bundesministerium für Forschung und Technologie (UC/FKW 23) is gratefully acknowledged.

Registry No. Perhydroxyl, 3170-83-0; oxygen, 7782-44-7; atomic hydrogen, 12385-13-6.

Kinetics of $O(^3P_J)$ Reactions with H_2O_2 and O_3

P. H. Wine,* J. M. Nicovich, R. J. Thompson, and A. R. Ravishankara

Molecular Sciences Group, Engineering Experiment Station, Georgia Institute of Technology, Atlanta, Georgia 30332
(Received: January 17, 1983)

The kinetics of the reactions $O(^3P_J) + H_2O_2 \rightarrow$ products (k_1) and $O(^3P_J) + O_3 \rightarrow 2O_2$ (k_2) have been investigated as a function of temperature over the temperature ranges 298–386 and 237–377 K, respectively. $O(^3P_J)$ was produced in the absence of other reactive free radicals by 532-nm pulsed laser photolysis of O_3 and detected by time-resolved resonance fluorescence spectroscopy. The following Arrhenius expressions adequately describe the experimental results: $k_1 = (1.13 \pm 0.54) \times 10^{-12} \exp[-(2000 \pm 160)/T]$ and $k_2 = (5.6 \pm 2.1) \times 10^{-12} \exp[-(1950 \pm 110)/T]$ (units are cm^3 $molecule^{-1}$ s^{-1}, errors are 2σ).

Introduction

Bimolecular reactions between species in the O_x and HO_x families play a central role in the chemistry of the stratosphere. One of the least studied of this important class of reactions is that of $O(^3P_J)$ with hydrogen peroxide:

$$O(^3P_J) + H_2O_2 \rightarrow OH + HO_2 \quad (1a)$$

$$\rightarrow O_2 + H_2O \quad (1b)$$

Some information pertaining to the kinetics of reaction 1 has been reported by several groups.[1-4] However, in only one investigation[3] does it appear that reaction 1 was isolated from competing side reactions well enough to provide a meaningful determination of k_1 ($\equiv k_{1a} + k_{1b}$), and even in this case the results have been questioned because the reported A factor is lower than would be expected for an H atom abstraction reaction.[5] The present investigation was undertaken to definitively determine the rate coefficient k_1 as a function of temperature. In addition to reaction 1, the important stratospheric reaction

$$O(^3P_J) + O_3 \rightarrow 2O_2 \quad (2)$$

was also investigated. A wealth of kinetic data is already available for reaction 2,[6-12] and good agreement exists

(1) S. N. Foner and R. L. Hudson, *J. Chem. Phys.*, **36**, 2681 (1962).
(2) E. A. Albers, K. Hoyermann, H. Gg. Wagner, and J. Wolfrum, "Proceedings of the 13th International Symposium on Combustion", Combustion Institute, Pittsburgh, PA, 1971, pp 81–8.
(3) D. D. Davis, W. Wong, and R. Schiff, *J. Phys. Chem.*, **78**, 463 (1974).
(4) J. M. Roscoe, *Int. J. Chem. Kinet.*, **14**, 471 (1982).
(5) "Chemical Kinetics and Photochemical Data for Use in Stratospheric Modeling", Evaluation No. 5, JPL publication 82-57, 1982.

0022-3654/83/2087-3948$01.50/0

between five of the six most recent studies.[8-12] However, because the rate coefficient for reaction 2 is such a crucial input parameter in models of stratospheric chemistry, $k_2(T)$ must be defined as accurately as possible. Hence, additional temperature-dependent kinetic data are desirable.

Experimental Section

The apparatus was similar to one which has been described previously.[13] $O(^3P_J)$ was produced in the absence of other reactive radicals by 532-nm pulsed laser photolysis of O_3 and monitored by time-resolved resonance fluorescence spectroscopy. Second harmonic radiation from a Nd:YAG laser was used as the photolytic light source. The laser pulse width was 10 ns and the maximum attainable power at 532 nm was 200 mJ per pulse. The resonance lamp consisted of an electrodeless microwave discharge through a few torr of flowing UHP helium. The lamp output was filtered with a calcium fluoride window to prevent impurity emissions of $H(^2S)$ and $N(^4S)$ resonance radiation from entering the reactor. Fluorescence in the ^3P–^3S transitions at 130.2–130.6 nm was collected by a magnesium fluoride lens and imaged onto the photocathode of a solar blind photomultiplier. The photolysis laser beam, resonance radiation beam, and photomultiplier were mutually orthogonal to one another. Signals were obtained by using photon counting techniques in conjunction with multichannel scaling. For each decay rate measured, sufficient flashes were averaged to obtain a well-defined temporal profile over at least two and usually more than three $1/e$ times.

Two different reaction cells were employed in this investigation. One was constructed of Pyrex with a diameter of 4.5 cm and a length of 15 cm while the other was constructed of brass with a diameter of 3.8 cm and a length of 21 cm. The Pyrex cell was used only in studies at ambient temperatures whereas the brass cell, constructed with channels in its walls through which heating or cooling fluids from a thermostated bath could be circulated, was used for carrying out temperature-dependence studies. A copper–constantan thermocouple with a stainless-steel jacket was inserted (along the direction of flow) into the reaction zone through a vacuum seal, thus allowing measurement of the gas temperature under the precise pressure and flow rate conditions of the experiment. To prevent heterogeneous decomposition of H_2O_2 and/or O_3, the interior of the brass cell was coated with FEP Telfon and then overcoated with halocarbon wax.

All experiments were carried out under "slow-flow" conditions. Linear flow rates through the reactor ranged from 1.4 to 6.1 cm s^{-1} and the laser repetition rate was 1 Hz; hence, the gas mixture in the reaction cell was completely replaced every few laser shots. O_3 was flowed from a 12-L bulb containing a dilute O_3/N_2 mixture while an H_2O_2/N_2 mixture was generated by bubbling nitrogen through H_2O_2 at 298 K. The O_3/N_2 mixture, H_2O_2/N_2 mixture, and additional N_2 were premixed before entering the reactor. To prevent significant decomposition of H_2O_2, all components traversed by H_2O_2 between the bubbler and the reactor were Pyrex or Teflon with the exception of a few stainless-steel fittings. The needle valve and flowmeter in the H_2O_2 line were positioned so that N_2 flowed through these components before entering the bubbler.

In studies of reaction 2, the concentration of O_3 in the mixture exiting (or in some cases entering) the reactor was determined by UV absorption at 213.9 nm. A Zn hollow cathode lamp was used as the light source for the absorption measurements and a $^1/_4$-m monochromator was used to isolate the 213.9-nm line. The absorption cell was 48 cm long. The O_3 absorption cross section at 213.9 nm was taken to be 8.57×10^{-19} cm^2.[14] In studies of reaction 1, the same absorption setup was employed to monitor H_2O_2 but in this case the monochromator was tuned to transmit the 202.6-nm Zn^+ line. The H_2O_2 absorption cross section at 202.6 nm was taken to be 4.30×10^{-19} cm^2.[15,16] An additional 10-cm absorption cell was also employed to monitor O_3 at 253.7 nm. An Hg pen ray lamp was used as the light source for this measurement and a band-pass filter was used to isolate the 253.7-nm line. The O_3 absorption cross section at 253.7 was taken to be 1.12×10^{-17} cm^2.[13] For the concentrations of H_2O_2 and O_3 employed to study reaction 1, H_2O_2 absorption was very small compared to O_3 absorption at 253.7 nm while the reverse was true at 202.6 nm. Hence, errors in the determination of $[H_2O_2]$ were eliminated through the use of two absorption cells.

The nitrogen diluent gas used in this study had a stated purity of ≥99.999%; it was used as supplied; 90% H_2O_2 (by weight) was obtained from FMC Corp. It was further concentrated by bubbling N_2 through it for several days before experiments were undertaken and constantly (24 h per day) during the course of experiments. O_3 was prepared by passing UHP O_2 (stated purity ≥ 99.99%) through a commercial ozonator and stored on silica gel at 197 K. Before use it was degassed at 77 K to remove O_2.

Results

Reaction 1 was more difficult to study than reaction 2 because photolyte (O_3) concentrations had to be kept low and because, at the H_2O_2 levels required to observe a reaction, significant absorption of $O(^3P_J)$ resonance radiation occurred; hence, signal levels were much lower than those obtainable in studying reaction 2. Due to the slow reaction rate, low signal levels, and low vapor pressure of H_2O_2, meaningful results could not be obtained below ambient temperatures. At temperatures around 390 K both H_2O_2 decomposition and deposition of halocarbon wax on cell windows became problems. Hence, reaction 1 could be studied only over the limited temperature range 298–386 K. Reaction 2 was investigated over the temperature range 238–377 K.

Both reactions 1 and 2 were investigated under pseudo-first-order conditions with $[R] \gg [O(^3P_J)]$, R = H_2O_2,

(6) For a review of pre-1969 data on reaction 2 see H. I. Schiff, *Can. J. Chem.*, **47**, 1903 (1969).
(7) D. Husain, L. J. Kirsch, and R. J. Donovan, *J. Photochem.*, **1**, 69 (1972).
(8) D. C. Krezenski, R. Simonaitis, and J. Heicklen, *Int. J. Chem. Kinet.*, **3**, 467 (1971).
(9) J. L. McCrumb and F. Kaufman, *J. Chem. Phys.*, **57**, 1270 (1972).
(10) D. D. Davis, W. Wong, and J. Lephardt, *Chem. Phys. Lett.*, **22**, 273 (1973).
(11) G. A. West, R. E. Weston, Jr., and G. W. Flynn, *Chem. Phys. Lett.*, **56**, 429 (1978).
(12) I. Arnold and F. J. Comes, *Chem. Phys.* **42**, 231 (1979).
(13) P. H. Wine and A. R. Ravishankara, *Chem. Phys.*, **69**, 365 (1982).
(14) N. Nicolet, "Etude des Reactions Chimiques de l'Ozone dans la Stratosphere", Institut Royal Meteorologique de Belgique, Brussels, 1980, pp 49–65.
(15) C. L. Lin, N. K. Rohatgi, and W. B. DeMore, *Geophys. Res. Lett.*, **5**, 113 (1978).
(16) L. J. Molina and M. J. Molina, *J. Photochem.*, **15**, 97 (1981).
(17) G. Kistiakowsky, *Z. Phys. Chem.*, **117**, 348 (1925).
(18) E. Castellano and H. J. Schumacher, *Z. Phys. Chem. (Frankfurt am Main)*, **34**, 198 (1962).
(19) W. D. McGrath and R. G. W. Norrish, *Proc. R. Soc. London, Ser. A*, **242**, 265 (1957).
(20) D. M. Ellis, J. J. McGarvey, and W. D. McGrath, *Nature (London), Phys. Sci.*, **229**, 153 (1971).
(21) R. V. Fitzsimmons and E. J. Bair, *J. Chem. Phys.*, **40**, 451 (1964).

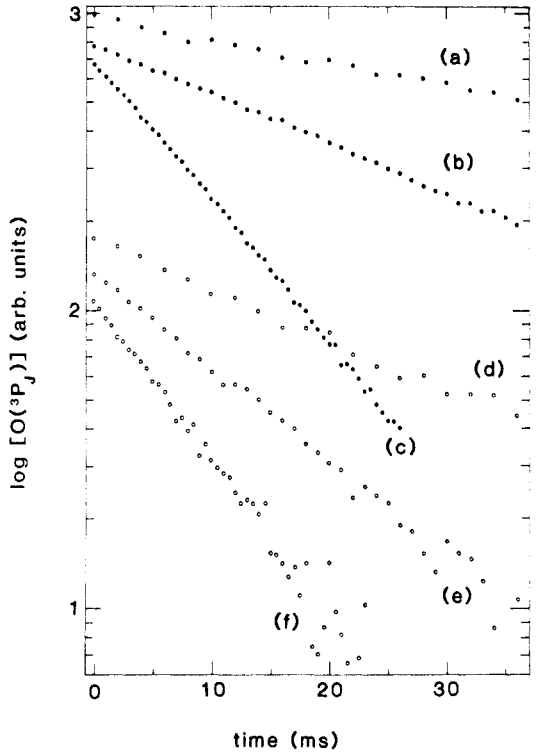

Figure 1. Typical $O(^3P_J)$ temporal profiles. Traces a–c are data for $O(^3P_J) + O_3$ at $T = 298$ K, $P = 100$ torr, $[O_3]/[O(^3P_J)]_0 = 10400$; $[O_3]$ in units of 10^{15} molecules cm^{-3} = (a) 1.53, (b) 5.92, (c) 19.3, number of laser shots averaged = (a) 128, (b) 100, (c) 200; k' values obtained from the data are (a) 16.6, (b) 38.2, and (c) 115 s^{-1}. The slight nonexponentiality observed in trace (c) results from nonlinearity in the $O(^3P_J)$ detection scheme at the high initial atom concentration of 2×10^{12} cm^{-3}. Traces d–f are data for $O(^3P_J) + H_2O_2$ at $T = 353$ K, $P = 100$ torr, $[O_3] = 7.0 \times 10^{14}$ cm^{-3}, $[O(^3P_J)]_0 = 1.7 \times 10^{11}$ cm^{-3}; $[H_2O_2]$ in units of 10^{15} molecules cm^{-3} = (d) 0.844, (e) 9.20, (f) 23.1; number of laser shots averaged = (d) 64, (e) 300, (f) 1500; k' values obtained from the data are (d) 37.7, (e) 73.1, and (f) 124 s^{-1}.

O_3. Therefore, under experimental conditions where the only processes which influence the $O(^3P_J)$ temporal profile are

$$O_3 \xrightarrow[532\text{ nm}]{h\nu} O(^3P_J) + O_2 \quad (3)$$

$$O(^3P_J) + O_3 \rightarrow 2O_2 \quad (2)$$

$$O(^3P_J) + H_2O_2 \rightarrow \text{products} \quad (1)$$

$O(^3P_J) \rightarrow$ loss by diffusion from the detector field of view and reaction with background impurities (4)

simple first-order kinetics are obeyed:

$$\ln \{[O(^3P_J)]_0/[O(^3P_J)]_t\} = (k_1[H_2O_2] + k_2[O_3] + k_4)t \equiv k't \quad (5)$$

As eq 5 predicts, when $[H_2O_2] = 0$ (i.e., studies of reaction 2, exponential $O(^3P_J)$ decays and a linear dependence of k' on $[O_3]$ were observed under all experimental conditions investigated. Typical data are shown in Figures 1 and 2. Bimolecular rate coefficients, $k_2(T)$, obtained from the slopes of k' vs. $[O_3]$ plots were found to be invariant to factor of 6 changes in $[O_3]/[O(^3P_J)]_0$, thus demonstrating that biradical processes, such as reaction of $O(^3P_J)$ with a product of reaction 2 or with a photolytically produced radical, were unimportant. When $[H_2O_2]$ is varied at constant $[O_3]$ (i.e., studies of reaction 1), eq 5 predicts that exponential decays should be observed, that k' should depend linearly on $[H_2O_2]$, and that the slope of a k' vs. $[H_2O_2]$ plot should be independent of $[O(^3P_J)]_0$. While observed $O(^3P_J)$ temporal profiles were exponential under

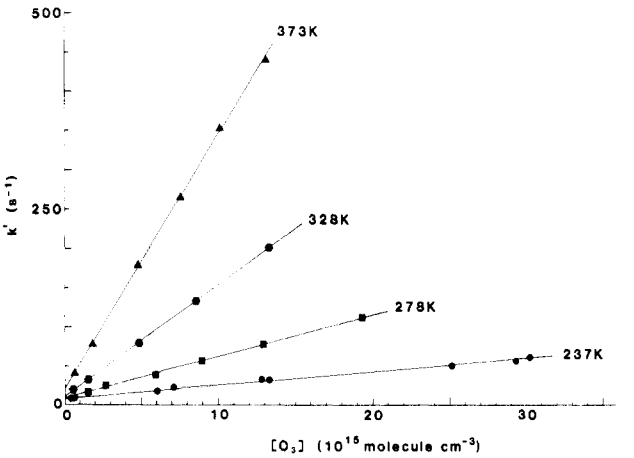

Figure 2. k' vs. $[O_3]$ plots at four temperatures. Rate coefficients for the reaction $O(^3P_J) + O_3 \rightarrow 2O_2$ are obtained from the slopes of these plots.

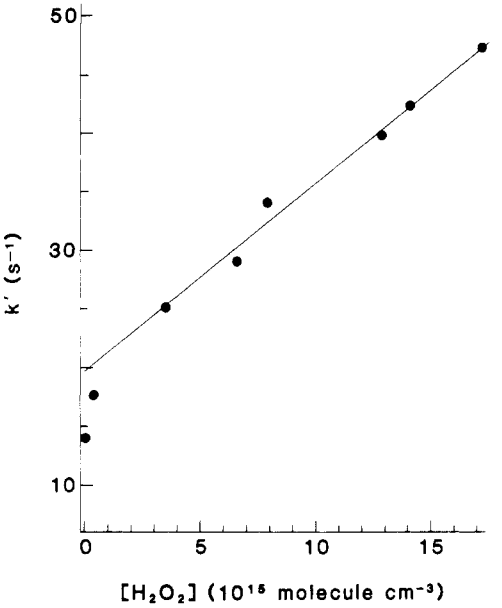

Figure 3. Typical k' vs. $[H_2O_2]$ plot. Rate coefficients for the reaction $O(^3P_J) + H_2O_2 \rightarrow$ products were obtained from the slopes of these plots using only data for $[H_2O_2] = 0.8 \times 10^{15}$ cm^{-3}. Experimental conditions used to obtain the data shown in the figure were as follows: $T = 298$ K, $P = 150$ torr, $[O_3] = 3.5 \times 10^{14}$ cm^{-3}, $[O(^3P_J)]_0 = 1.0 \times 10^{11}$ cm^{-3}. The solid line is obtained from an unweighted linear least-squares analysis of the six data points for which $[H_2O_2]$ is the highest. The rate coefficient ($k_1 \pm 2\sigma$) obtained from the data is $1.63 \pm 0.19 \times 10^{-15}$ cm^3 $molecule^{-1}$ s^{-1}.

most experimental conditions (Figure 1), other deviations from the desired behavior were observed. First, k' vs. $[H_2O_2]$ plots were found to be linear only for $[H_2O_2] > 0.8 \times 10^{15}$ molecules cm^{-3} (Figure 3). One possible explanation for the behavior observed at low $[H_2O_2]$ is that a small fraction of H_2O_2 underwent wall-catalyzed decomposition to yield a background HO_2 concentration of 10^{10}–10^{11} molecules cm^{-3}:

$$H_2O_2 \rightarrow 2OH \quad (6)$$

$$OH + H_2O_2 \rightarrow HO_2 + H_2O \quad (7)$$

The reaction

$$O(^3P_J) + HO_2 \rightarrow OH + O_2 \quad (8)$$

would then constitute an additional $O(^3P_J)$ removal mechanism of the observed magnitude which depended on the presence of H_2O_2. Another possibility is that H_2O_2 catalyzed removal of $O(^3P_J)$ at the reactor walls. It is

TABLE I: Summary of Kinetic Data for the Reaction $O(^3P_J) + H_2O_2 \xrightarrow{k_1}$ Products

T, K	P, torr	$10^{-11}[O(^3P_J)]_0$, molecules cm^{-3}	range of k', s^{-1}	$10^{15}k_1^{app}$,[a] cm^3 molecule^{-1} s^{-1}	$10^{15}k_1$,[b] cm^3 molecule^{-1} s^{-1}
298	100	0.43	19.7-48.6	1.36 ± 0.11	
	150	4.3	37.1-75.3	1.94 ± 0.20	
	150	7.6	41.8-88.1	2.16 ± 0.08	
	15	1.3	49.9-85.3	1.76 ± 0.20	
	150	1.0	25.1-47.5	1.63 ± 0.19	
	50	1.3	38.1-61.6	1.54 ± 0.10	
	100	2.0	28.0-65.7	1.65 ± 0.06	1.45 ± 0.29
312	100	0.41	19.0-61.0	1.82 ± 0.12	
	100	1.6	36.7-79.5	1.97 ± 0.07	
	100	57	62.0-146	3.32 ± 0.05[c]	
	100	6.8	43.1-96.1	2.32 ± 0.27	
	100	1.7	24.4-66.2	1.86 ± 0.10	1.79 ± 0.27
328	100	2.1	33.9-112	2.52 ± 0.08	2.52 ± 0.37
353	100	2.1	37.7-124	3.81 ± 0.13	3.81 ± 0.57
373	100	2.6	58.7-152	5.80 ± 0.56	5.80 ± 0.87
377	100	3.1	65.2-143	5.25 ± 0.59	5.25 ± 0.79
386	100	0.44	46.7-123	6.61 ± 0.80	6.61 ± 0.99

[a] Errors are 2σ and refer to precision only. [b] Errors represent estimates of overall accuracy. [c] Decays were nonexponential; k_1 estimated from data in first 10 ms after laser fired.

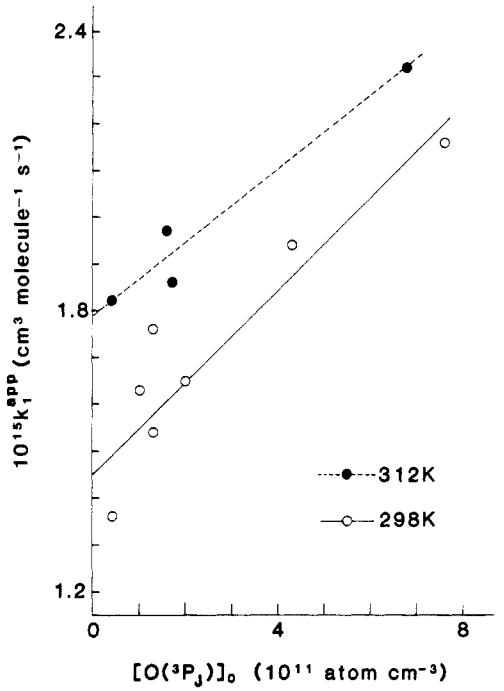

Figure 4. Plots of the apparent bimolecular rate coefficient vs. $[O(^3P_J)]_0$ for the reaction $O(^3P_J) + H_2O_2 \rightarrow$ products at 298 and 312 K. By extrapolation to $[O(^3P_J)]_0 = 0$, the rate coefficients are found to be 1.45×10^{-15} cm^3 molecule^{-1} s^{-1} at 298 K and 1.79×10^{-15} cm^3 molecule^{-1} s^{-1} at 312 K.

unusual for diffusion of radicals back from the reactor walls to be important in flash photolysis experiments. However, the system geometry and slow observed background $O(^3P_J)$ loss rate (~ 8 s^{-1}) in these experiments are more favorable for wall effects to be important than is typically the case. The process responsible for the observed k' vs. $[H_2O_2]$ behavior apparently saturated at $[H_2O_2] \sim 0.8 \times 10^{15}$ molecules cm^{-3} and contributed ~ 5 s^{-1} to the rate coefficient k_4. Since signal-to-noise considerations limited the maximum $k' - k_4$ which could be measured at 298 K to ~ 50 s^{-1}, a contribution of 5 s^{-1} could not simply be ignored on the grounds of being negligible. Only data obtained for $[H_2O_2] > 0.84 \times 10^{15}$ molecules cm^{-3} were used to determine k_1. Another kinetic complication observed in studies of reaction 1 is that, at the lower temperatures studied, the slopes of k' vs. $[H_2O_2]$ plots (slope $\equiv k_1^{app}$) were not independent of $[O(^3P_J)]_0$, but instead showed a tendency

TABLE II: Summary of Kinetic Data for the Reaction $O(^3P_J) + O_3 \xrightarrow{k_2} 2O_2$

T, K	P, torr	$[O_3]/[O(^3P_J)]_0$	range of k' s^{-1}	$10^{15}k_2$,[a] cm^3 molecule^{-1} s^{-1}
237	100	11 700	8.9-60.9	1.67 ± 0.16
	100	1 940	8.1-55.2	1.64 ± 0.03
249	100	9 380	9.4-68.3	2.16 ± 0.13
255	100	9 380	12.6-72.1	2.07 ± 0.06
261	100	10 400	20.3-110	3.79 ± 0.12
278	100	10 400	16.6-111	5.28 ± 0.21
297	150		21.5-150	8.78 ± 0.47
	150	21 700	24.0-207	8.14 ± 0.30
	50	11 700	20.0-176	8.15 ± 0.34
	150	9 970	21.4-135	7.70 ± 0.25
302	15	11 300	42.0-104	8.52 ± 0.47
328	100	9 370	19.8-200	14.2 ± 0.1
350	100	10 400	29.6-329	20.5 ± 0.5
373	100	10 400	41.0-440	32.3 ± 0.7
377	100	11 600	51.8-473	33.7 ± 4.7

[a] Errors are 2σ and refer to precision only.

to increase with increasing $[O(^3P_J)]_0$. We believe that the secondary reaction of $O(^3P_J)$ with HO_2, i.e., reaction 8, contributed significantly to $O(^3P_J)$ removal under conditions where $k_8[HO_2]/k_1[H_2O_2]$ is maximized—high $[O(^3P_J)]_0$ and low temperature. Plots of k_1^{app} vs. $[O(^3P_J)]_0$ for data at 298 and 312 K are shown in Figure 4. The reported values for k_1 at 298 and 312 K are obtained from linear extrapolations of the k_1^{app} vs. $[O(^3P_J)]_0$ data to $[O(^3P_J)]_0 = 0$. As a result, the uncertainty in k_1 (298 K) is somewhat higher than the uncertainties in k_1 (T) values at higher temperatures. A more detailed discussion of the secondary chemistry encountered in studies of reaction 1 is given later in the paper.

For both reactions 1 and 2 measured bimolecular rate coefficients were found to be independent of which reaction cell was employed and also independent (at both low and high temperature) of whether the reaction mixture flowed through the absorption cell after leaving the reactor or before entering the reactor. These observations prove that the measured reactant concentrations accurately reflected the actual concentrations in the reactors. As expected, both k_1 and k_2 were found to be independent of total N_2 pressure over the range 15–150 torr. Kinetic data for reactions 1 and 2 are summarized in Tables I and II. Errors quoted in Table I for individual determinations of k_1^{app} and in Table II for individual determinations of k_2 are 2σ and refer to precision only. The overall accuracy

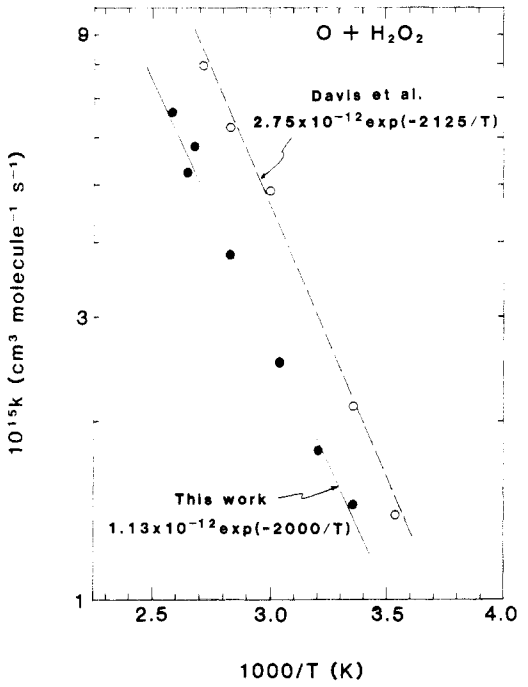

Figure 5. Arrhenius plot for the reaction $O(^3P_J) + H_2O_2 \rightarrow$ products. Both our data and the data of Davis et al. (ref 3) are shown. The solid line is obtained from an unweighted linear least-squares analysis of our data. The dashed line is a reproduction of the Arrhenius expression reported by Davis et al.

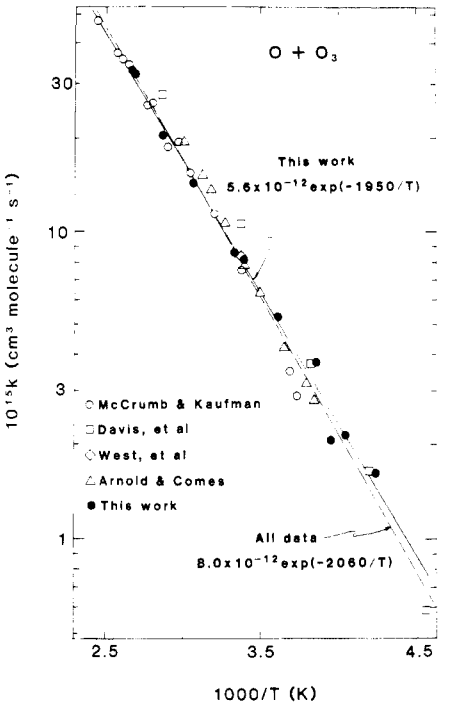

Figure 6. Arrhenius plot for the reaction $O(^3P_J) + O_3 \rightarrow 2O_2$. All data reported in this study and in ref 9–12 are included in the plot. The lines are obtained from unweighted linear least-squares analyses of our data (solid line) and all data (dashed line).

of each $k_1(T)$ is estimated to be ±15% except ±20% for k_1 (298 K), while the overall accuracy of each $k_2(T)$ is estimated to be ±10%. Arrhenius plots of the results for reactions 1 and 2 are shown in Figures 5 and 6. Unweighted linear least-squares analyses give the following Arrhenius expressions:

$$k_1 = (1.13 \pm 0.54) \times 10^{-12} \exp[-(2000 \pm 160)/T]$$

$$k_2 = (5.6 \pm 2.1) \times 10^{-12} \exp[-(1950 \pm 110)/T]$$

Errors in the Arrhenius parameters are 2σ and refer to precision only ($\sigma_A \equiv A\sigma_{\ln A}$).

Discussion

Since evidence for secondary removal of $O(^3P_J)$ was observed in our study of reaction 1, a quantitative discussion of contributions from secondary reactions seems to be in order. A prerequisite for such a discussion is a reasonably accurate knowledge of the concentration of $O(^3P_J)$ produced via photolysis of O_3. The values of $[O(^3P_J)]_0$ given in Table I were computed on the basis of known O_3 concentrations, an O_3 absorption cross section at 532 nm of 1.3×10^{-21} cm^2,[14] and laser photon fluences determined by measuring the diameter (d) of an iris which was adjusted to transmit 50% of the (expanded beam) laser power and then dividing the transmitted power by $\pi d^2/4$. In one set of experiments where a very high $[O(^3P_J)]_0$ was desired, the unexpanded laser beam was employed and the beam diameter was obtained from a Polaroid burn pattern. It should be noted that, since the photolysis laser beam was not spatially uniform in intensity, the determined values of $[O(^3P_J)]_0$ are only approximate, with estimated uncertainties being ±30%.

As a worst case scenario, we consider the case where reaction 1 proceeds entirely via channel 1a. Then for each $O(^3P_J)$ consumed, two HO_2 molecules are formed:

$$O(^3P_J) + H_2O_2 \rightarrow OH + HO_2 \quad (1a)$$

$$OH + H_2O_2 \rightarrow HO_2 + H_2O \quad (7)$$

Since k_7/k_1 is approximately 1000,[5] reaction 7 is virtually instantaneous on the time scale for $O(^3P_J)$ removal. Under the conditions employed in our experiments, HO_2 removal by the reactions

$$HO_2 + O_3 \rightarrow OH + 2O_2 \quad (9)$$

$$HO_2 + HO_2 \rightarrow O_2 + H_2O_2 \quad (10)$$

is expected to be negligibly slow. Similarly, since the steady-state concentration of OH is very small, the reactions

$$OH + HO_2 \rightarrow O_2 + H_2O \quad (11)$$

$$OH + O(^3P_J) \rightarrow O_2 + H(^2S) \quad (12)$$

are unimportant. Based on known kinetic information,[5] the dominant secondary reaction should be reaction 8. Recent measurements[22-24] indicate that $k_8(298\ K) \sim 6.0 \times 10^{-11}$ cm^3 molecule^{-1} s^{-1} and reaction 8 proceeds with little or no activation energy. In keeping with our worst case scenario, we assume that background removal of HO_2 is negligibly slow, i.e., $k_{13} = 0$

$$HO_2 \rightarrow \text{loss by diffusion from detector field of view and reaction with background impurities} \quad (13)$$

and that $[H_2O_2] \gg [O_3]$ so all $O(^3P_J)$ is consumed via reaction 1a. Then, if $[O(^3P_J)]_0 = 1 \times 10^{11}$ molecules cm^{-3}, after 80% of $O(^3P_J)$ has been consumed, 1.6×10^{11} HO_2 cm^{-3} will be present. Under these conditions $k_8[HO_2] \sim 10$ s^{-1}. Since all measurements of k_1 at 298 K were carried out under conditions where $k_1[H_2O_2]$ was less than 50 s^{-1}, it is clear that even at the lowest $[O(^3P_J)]_0$ employed, i.e., 4.3×10^{10} molecules cm^{-3}, small contributions from reac-

(22) L. F. Keyser, *J. Phys. Chem.*, **86**, 3439 (1982).
(23) U. C. Sridharan, L. X. Qui, and F. Kaufman, *J. Phys. Chem.*, **86**, 4569 (1982).
(24) A. R. Ravishankara, P. H. Wine, and J. M. Nicovich, *J. Chem. Phys.*, **78**, 6629 (1983).

TABLE III: Comparison of Our Results for the Reaction $O(^3P_J) + H_2O_2 \xrightarrow{k_1}$ Products with Those Reported by Other Investigators

investigators	ref	range of T, K	$10^{12}A \pm 2\sigma$, cm^3 molecule^{-1} s^{-1}	$E/R \pm 2\sigma$, K	$10^{15}k_1$,[a] cm^3 molecule^{-1} s^{-1} 298 K	220 K
Foner and Hudson	1	298			<4	
Albers, Hoyermann, Wagner, and Wolfrum	2	370-800	46.5	3220 ± 300	0.943	0.0205
Davis, Wong, and Schiff	3	283-368	2.75 ± 0.41	2125 ± 261	2.20	0.176
recommendation of NASA and CODATA panels[b]	5, 24		10	2500 ± 1000	2.27	0.116
this work		298-386	1.13 ± 0.54	2000 ± 160	1.38	0.127

[a] Where T-dependent data are reported, rate coefficients are calculated from Arrhenius parameters. [b] Based on the 298 K data of Davis et al. and an assumed A factor of 1×10^{-11} cm^3 molecule^{-1} s^{-1}.

tion 8 are possible. It does appear, however, that using the extrapolation procedure outlined earlier (Figure 4), we have obtained a measurement of k_1 which is free of contributions from unwanted side reactions.

Despite the apparent simplicity of the chemistry occurring in the reaction mixtures employed to study reaction 2, there are potential complications which need to be addressed. Two O_3 photolysis channels are energetically allowed at 532 nm

$$O_3 \rightarrow O(^3P_J) + O_2(X^3\Sigma_g^-) \quad (3a)$$

$$\rightarrow O(^3P_J) + O_2(a^1\Delta_g) \quad (3b)$$

$O_2(a^1\Delta_g)$ reacts with O_3 to produce $O(^3P_J)$

$$O_2(a^1\Delta_g) + O_3 \rightarrow 2O_2 + O(^3P_J) \quad (14)$$

with k_{14} being about half the measured value for k_2.[5] Hence, if a significant fraction of photolysis events occurred via channel 3b, k_2 would be underestimated. Channel 3b is spin forbidden and, therefore, is unlikely to be a major photodissociation pathway. Fortunately, there is experimental evidence in the literature which supports this contention. Classical photochemical studies[17,18] have demonstrated that, when photolyzing light is restricted to $\lambda > 411$ nm (the energetic onset for $O(^1D_2)$ production), the quantum yield for ozone destruction never exceeds 2.1. Hence, it appears that channel 3b cannot account for more than a few percent of O_3 photolysis events.

Reaction 2 is highly exothermic [$\Delta H = 93.7$ kcal mol^{-1}). Hence, both $O_2(a^1\Delta_g)$ and $O_2(b^1\Sigma_g^+)$ are energetically accessible products. Like $O_2(a^1\Delta_g)$, $O_2(b^1\Sigma_g^+)$ reacts with O_3 to produce $O(^3P_J)$

$$O_2(b^1\Sigma_g^+) + O_3 \rightarrow 2O_2 + O(3P_J) \quad (15)$$

with reaction 15 being much faster than reactions 2 and 14.[5] Therefore, if $O_2(b^1\Sigma_g^+)$ were formed with a significant yield, k_2 would be underestimated. Formation of $O_2(a^1\Delta_g)$ as a product of reaction 2 could also lead to underestimation of k_2, but in this case the kinetic complication would manifest itself as an nonexponential $O(^3P_J)$ decay. The classical photochemical results alluded to above strongly suggest that neither $O_2(a^1\Delta_g)$ nor $O_2(b^1\Sigma_g^+)$ is formed as a product of reaction 1. Furthermore, flash photolysis studies have demonstrated directly that most of the reaction 2 exothermicity goes into vibrational excitation of $O_2(X^3\Sigma_g^-)$[19,20] and that vibrational relaxation, even in pure O_3, proceeds via a stepwise mechanism with no resultant O_3 decomposition.[21]

Our results for reaction 1 are compared with those reported by other investigators in Table III. The Arrhenius expression currently recommended by both the NASA[5] and CODATA[25] panels is also included in Table III. The recommended rate expression is based on the 298 K data of Davis et al.[3] and an assumed A factor of 1×10^{-11} cm^3 molecule^{-1} s^{-1}, an A factor which would be expected for an atom–molecule abstraction reaction such as channel 1a. Interestingly, the activation energy that we obtain agrees well with that reported by Davis et al. but the A factor obtained from our data is significantly lower than Davis et al.'s (Figure 5) and about 1 order of magnitude lower than the "expected" value. The somewhat higher activation energy reported by Albers et al.[2] for data obtained over the temperature range 370–800 K suggests the possibility that the dependence of ln k on $1/T$ is not linear. Interestingly, Albers et al. report some data at $T < 370$ K which do suggest a lower activation energy at lower temperatures. A nonlinear ln k vs. $1/T$ dependence would not be at all surprising, particularly since reaction 1 has two possible sets of products and can proceed via initial attack at either an H atom or an O atom. It should be noted that use of available Arrhenius expressions for $k_1(T)$ would lead to underestimation of k_1 at stratospheric temperatures if the activation energy does, indeed, decrease with decreasing temperature.

At least some of the difference between the rate coefficients reported by Davis et al.[3] and those obtained in this study probably results from the fact that reaction 8 contributed significantly to $O(^3P_J)$ removal in Davis et al.'s experiments. Davis et al. report that measured pseudo-first-order decay rates were independent of a factor of 5 variation in laser power although actual laser photon fluences are not given in their paper. Our results (Figure 4) indicate that increasing $[O(^3P_J)]_0$ from 1×10^{11} to 5×10^{11} molecules cm^{-3} results in approximately a 25% increase in k_1^{app} at 298 K. In Davis et al.'s experiments reaction with O_3 and diffusion from the detector field of view accounted for half the $O(^3P_J)$ removal at the highest H_2O_2 concentrations employed and an even greater fraction at lower H_2O_2 levels. Hence, in their experiments a 25% change in k_1 would result in a change of ≤12% in measured pseudo-first-order rate coefficients. Given the poor signal-to-noise ratio inherent in resonance fluorescence detection of $O(^3P_J)$ in the presence of large concentrations of H_2O_2, it does not seem too surprising that a 12% variation in k' with varying laser power would have gone unnoticed. Another potential problem in Davis et al.'s experiments arises from the fact that these authors did not measure the H_2O_2 concentration in situ in the (static) reactor. Small corrections were made for heterogeneous decomposition of H_2O_2; these corrections were based on independent photometric measurements of the H_2O_2 disappearance rate in temperature-controlled Pyrex cells. If

(25) D. L. Baulch, R. A. Cox, P. J. Crutzen, R. F. Hampson, Jr., J. A. Kerr, J. Troe, and R. T. Watson, *J. Phys. Chem. Ref. Data*, 11, 327 (1982).

TABLE IV: Comparison of Our Results for the Reaction $O(^3P_J) + O_3 \xrightarrow{k_2} 2O_2$ with Those Reported by Other Investigators[d]

investigators	ref	range of T, K	$10^{12}A \pm 2\sigma$, cm^3 molecule^{-1} s^{-1}	$E/R \pm 2\sigma$, K	$10^{15}k_2$,[a] cm^3 molecule^{-1} s^{-1} 298 K	220 K
Husain, Kirsch, and Donovan	7	300			13 ± 5	
McCrumb and Kaufman	9	269-409	10.5 ± 3.6	2170 ± 100	7.22	0.546
Davis, Wong, and Lephardt	10	220-353	20.2 ± 3.8	2276 ± 208	9.74	0.649
West, Weston, and Flynn	11	298			8.3 ± 0.6	
Arnold and Comes	12	262-335	21.2 ± 3.6	2337 ± 52	8.33	0.516
this work		237-377	5.6 ± 2.1	1950 ± 110	8.06	0.792
recommendation of NASA panel[b]	5		15	2218 ± 150	8.78	0.627
recommendation of CODATA panel[c]	24		18	2300	8.00	0.519
all data from ref 9-12 and this work		220-409	8.0 ± 2.0	2060 ± 80	7.96	0.686

[a] Where T-dependent data are reported, rate coefficients are calculated from Arrhenius parameters. [b] Based on the data reported in ref 9 and 10. [c] Based on the data reported in ref 9-12. [d] Only direct measurements reported since 1970 are tabulated.

the corrections were too large, Davis et al.'s rate coefficients could be overestimated by 1–10%, while if the corrections were too small their rate coefficients would be underestimated. Hence, it does not seem possible to account for the differences between our results and those of Davis et al. as being due to loss of H_2O_2 at the walls of their reactor. Decomposition during transfer from the sample reservoir to the reactor could also have been a problem in their experiments, but such a problem would also hae resulted in overestimation of $[H_2O_2]$ and, therefore, underestimation of $k_1(T)$.

Our results for reaction 2 are compared with those obtained in other direct studies in Table IV. Those results which are used as a basis for currently recommended rate constants[5,25] are indicated. Recommended rate constants are also included in the table. Our data and data from ref 9–12 are plotted in Arrhenius form in Figure 6. It is clear that, although our data yield a slightly lower activation energy and lower A factor than is obtained from the other three temperature-dependent studies,[9,10,12] individual data points are in good agreement in the overlapping temperature regimes. A linear least-squares analysis which equally weights each of the 39 data points in Figure 6 gives the following Arrhenius expression (errors are 2σ):

$$k_2 = (8.0 \pm 2.0) \times 10^{-12} \exp[-(2060 \pm 80)/T]$$

This expression predicts that $k_2 = 7.96 \times 10^{-15}$ cm^3 molecule^{-1} s^{-1} at 298 K and 6.86×10^{-16} cm^3 molecule^{-1} s^{-1} at 220 K (a temperature typical of the lower stratosphere).

Estimates of the branching ratio for reaction 1 have been reported by Albers et al.[2] and Roscoe.[4] Albers et al. studied reaction 1 under conditions where the OH and HO_2 products of reaction 1a were rapidly removed by reaction with $O(^3P_J)$. They obtained for the overall stoichiometry of reactions 1, 8, and 12 the relationship

$$H_2O_2 + 2.5O(^3P_J) \rightarrow 2O_2 + 0.5H_2O + H(^2S) \quad (16)$$

from which they concluded that $k_{1a}/k_1 \sim 0.5$. Roscoe also studied reaction 1 in a flow system under conditions where $O(^3P_J)$ removal was dominated by secondary reactions.[4] Using a 10-reaction scheme he modeled his results and those of Albers et al.[2] and Davis et al.[3] and concluded that the data are best explained if it is assumed that k_{1a}/k_1 is unity. It is, in principle, possible to obtain information about the branching ratio for reaction 1 by examining the dependence of $O(^3P_J)$ temporal profiles on $[O(^3P_J)]_0$ since the free-radical products of reaction 1a rapidly consume $O(^3P_J)$ while the stable products of reaction 1b are relatively unreactive toward $O(^3P_J)$. Our experiments at T = 312 K, in which $[O(^3P_J)]_0$ was varied by a factor of 140, were carried out with the idea of using the results to estimate k_{1a}/k_1. A seven-reaction scheme—reactions 1, 2, 4, 7, 8, 10, and 13—was used to model the observed temporal profiles. The rate equations were solved numerically. Our results for k_1, k_2, and k_4 were used in the calculations along with values for k_7, k_8, and k_{10} recommended by the NASA panel.[5] k_{13} and k_{1a}/k_1 were treated as adjustable parameters with k_{13} varied from 0 to $2k_4$ and k_{1a}/k_1 varied from 0 to 1. For all temporal profiles investigated, the data were best reproduced by assuming values for k_{1a}/k_1 in the range 0.4–0.8. However, when uncertainties in $[O(^3P_J)]_0$, k_8, and k_{13} are taken into account, a value for k_{1a}/k_1 near unity cannot be completely ruled out. The only conclusion that we can draw with certainty concerning the branching ratio for reaction 1 is that $k_{1a}/k_1 > 0.2$.

In the absence of unaccounted for systematic errors in our data, we can confidently place an upper limit of 2.5×10^{-12} cm^3 molecule^{-1} s^{-1} on the A factor for reaction 1. Whatever the branching ratio for reaction 1 and, in fact, whether the reactive site in H_2O_2 is an H atom or an O atom, one would predict that the A factor for reaction 1 should be $\geq 1 \times 10^{-11}$ cm^3 molecule^{-1} s^{-1}. Entropy considerations suggest that the observed A factor implies an unusually "tight" transition state involving very close interaction distances and/or a critical geometry. It is worth noting that the A factor for the reaction of OH with H_2O_2, 3.1×10^{-12} cm^3 molecule^{-1} s^{-1},[5] is also considerably lower than would have been predicted.

Acknowledgment. We acknowledge Professor W. L. Chameides and Dr. D. M. Golden for helpful discussions. This work was supported by the National Aeronautics and Space Administration through subcontract No. 954814 from the Jet Propulsion Laboratory.

Registry No. O_3, 10028-15-6; H_2O_2, 7722-84-1; O, 17778-80-2.